

CIF2WAN: A Tool to Generate Input Files for Electronic Structure Calculations with Wannier90

Christopher Sims¹

*Department of Physics, University of Central Florida, Orlando, Florida 32816,
USA*^{a)}

The generation of input files for density functional theory (DFT) programs must often be manually done by researchers. If one wishes to produce a maximally localized wannier functions (MLWFs) the calculation consists of several separate files that must be formatted correctly in order for the program to work properly. Many of the inputs are repeated throughout the files and can be easily automated. In this work, a program is presented to generate all of the input files needed to produce wannier functions with Wannier90 starting from open source DFT programs such as Quantum espresso, Abinit, and Siesta. In addition, the input files for WannierTools are also included for those that wish to produce surface green's functions for the generation of surface state bands. The program presented allows for users new to DFT to use the programs with minimal understanding of parameters needed to produce good results, in addition, this program allows for researchers who are advanced DFT users to utilize this program for high throughput wannier calculations.

I. PROGRAM SUMMARY

Program title: CIF2WAN

Licensing provisions: GNU General Public Licence 3.0

Program obtainable from: Programming language:
Python

Has the code been vectorised or parallelized?: no

Computer: Any computer that can run Python v3.6+

Operating system: Any operating system that can run Python v3.6+

external libraries: numpy, pymatgen (w/ registration),
glob, shutil, csv

Running time: less than a minute (DFT runs are
separate)

Wannier90¹⁶. With these programs on is able to calculate surface band structures utilizing the iterative surface green function matching technique such as the method implemented in Wannier tools¹⁷ or chinook¹⁸. The main issue with DFT, especially if one wishes to conduct high throughput calculation is that one must meticulously format the input files for DFT programs so that there is no error in the calculation. Small errors cannot bypass the error detection built into DFT programs and learning the best methods for input will take some time for a beginner. Rather, having programs that assist in the pre-processing stage are more favorable for *ab initio* DFT theorists. While tools such as CIF2CELL¹⁹, Aiida²⁰, pymatgen²¹, jarvis^{22–27}, etc. exist, non can generate all of the input files needed to generate the wannier tight binding (TB) Hamiltonian utilizing multiple different quantum chemistry programs.

Recently, there has been a rising interest in identifying materials by their surface states. This began with the discovery of a 3D topological insulator which was confirmed by angle-resolved photoemission spectroscopy and density functional theory^{28–30}. Later, nodal-line and Weyl semimetal states have been discovered in real crystal systems such as ZrSiS^{31–34} and TaAs^{35–37}, respectfully. All of these materials are confirmed to be topologically non-trivial via berry phase, wannier charge center, or Wilson loop analysis. All of these methods can be performed with wannier functions. However, in order to properly perform calculations of a large amount of materials that can be topologically non-trivial will require many input files to various DFT programs. The automation of these tasks will make these calculations much simpler to perform.

This work presents CIF2WAN, a python program that can generate the input files in order to perform wannier calculations from *ab initio* calculations. In addition, slurm job handling files which are common in most supercomputer clusters are also generated for the user. The goal of this program is to make DFT calculations that utilize wannier TB Hamiltonians easier to understand for beginners and easier for more advance users of DFT programs.

^{a)}Christopersims@knights.ucf.edu

III. METHODS

Wannier functions can be seen as a derivation of the bloch function with an associated phase factor $e^{-i\mathbf{k}\cdot\mathbf{R}}$ is the real space lattice vector. In addition, one can label each band with its associated real space lattice vector \mathbf{R}_n where n is the band index. With this we can construct the wannier functions for each band index n .³⁸

$$|\mathbf{R}_n\rangle = \frac{V}{(2\pi)^3} \int_{BZ} d\mathbf{k} e^{-i\mathbf{k}\cdot\mathbf{R}} |\Psi_{n\mathbf{k}}\rangle \quad (1)$$

In order to compute wannier functions one must introduce a unitary mixing parameter $U_{mn}^{\mathbf{k}}$ to make the Hamiltonian smooth in all of k-space

$$|\mathbf{R}_n\rangle = \frac{V}{(2\pi)^3} \int_{BZ} d\mathbf{k} e^{-i\mathbf{k}\cdot\mathbf{R}} \sum_{m=1}^J U_{mn}^{\mathbf{k}} |\Psi_{m\mathbf{k}}\rangle \quad (2)$$

A common way to compute the wannier functions is via the projection method. Starting from a set of trial projections (J), These trial functions are projected onto the Bloch manifold.

$$|\psi_{n\mathbf{k}}\rangle = \sum_{m=1}^J |\Psi_{m\mathbf{k}}\rangle \langle \Psi_{m\mathbf{k}}| g_n \quad (3)$$

In order to do this calculation the matrix of inner products must first be computed. $(A_{\mathbf{k}})_{mn} = \langle \Psi_{m\mathbf{k}} | g_n \rangle$. By substituting this into equation 3, one can construct the trial wannier functions that are related to the real Bloch functions.

$$|\tilde{\psi}_{n\mathbf{k}}\rangle = \sum_{m=1}^J |\Psi_{m\mathbf{k}}\rangle (S_{\mathbf{k}}^{-1/2})_{mn} \quad (4)$$

Using these equations one can then minimize the localization function Ω

$$\Omega = \sum_n [\langle \mathbf{0}_n | r^2 | \mathbf{0}_m \rangle - \langle \mathbf{0}_n | \mathbf{r} | \mathbf{0}_m \rangle^2] = \sum_n [r^2 - \tilde{r}_n^2] \quad (5)$$

MLWFs can be derived by minimizing this function for each k point in the lattice with respect to $U_{mn}^{\mathbf{k}}$ after the bands have been calculated during the self consistent step of a DFT calculation. This procedure is repeated until $\Delta\Omega$ is sufficient small.¹³

IV. FEATURES OF CIF2WAN

CIF2WAN generates all of the input files needed to start from *ab initio* calculations in ABINIT, Quantum ESPRESSO, etc. to the generation and use of the wannier tight binding Hamiltonian (seedname_hr.dat) used in wannier tools. The program can load these files utilizing either a CIF file or by directly interfacing with materials project via pymatgen. The output is as follows for the following DFT programs.

V. INSTALLATION AND USAGE

In this section, we present how to install and use CIF2WAN.

TABLE I. Output for Quantum ESPRESSO

File	Description
seedname.scf.in	self consistent input file
seedname.nscf.in	Non-self consistent input file
seedname.p2w.in	input file for PW2Wannier90
seedname.win	input file for wannier90
scf.slurm	scf slurm file
nscf.slurm	nscf slurm file
p2w.slurm	p2w slurm file
wann.slurm	wann slurm file
cleandft.sh	cleanup for another DFT run
PP/	Pseudopotential folder
WT/	wanniertools folder
WT/wt.in	wanniertools input file
WT/wt.slurm	wanniertools slurm input file

TABLE II. Output for ABINIT

File	Description
seedname.in	ABINIT input file
seedname.files	file linking for ABINIT
seedname.slurm	main slurm file
w90.win	input file for wannier90
cleandft.sh	cleanup for another DFT run
PP/	Pseudopotential folder
WT/	wanniertools folder
WT/wt.in	wanniertools input file
WT/wt.slurm	wanniertools slurm input file

TABLE III. Output for VASP

File	Description
PBE/	Folder for PBE run
HSE06/	Folder for HSE run
W90/	Folder for W90 run
KPOINTS	Global, K points
POSCAR	Global, crystal information
PBE/INCAR	INCAR for PBE
HSE06/INCAR	INCAR for HSE06
W90/INCAR	INCAR for W90
vsp.slurm	main slurm file
wannier90.win	input file for wannier90
WT/	wanniertools folder
WT/wt.in	wanniertools input file
WT/wt.slurm	wanniertools slurm input file

TABLE IV. Output for SIESTA

File	Description
seedname.fdf	main input file
*.psf	pseudo for atoms
wannier90.win	input file for wannier90
cleandft.sh	cleanup for another DFT run
WT/	wanniertools folder
WT/wt.in	wanniertools input file
WT/wt.slurm	wanniertools slurm input file

A. Get CIF2WAN

CIF2WAN is an open source software package distributed under the GNU General Public license 3.0 (GPL). The code can be downloaded directly from the public code repository: <https://github.com/ChristopherSims/CIF2WAN>.

B. Installation and running the code

The code requires no installation, in the future this package may be developed into a python package. The version of python must be 3.6 or higher, in addition the user must install the following python packages: pymatgen, matplotlib, numpy, string, shutil, csv. These programs will likely automatically install in most modern python CDEs. In addition, one must obtain an APIKEY for usage of pymatgen (only if one uses the PYMATGEN flag), this key can be obtained by registering an account at materialsproject.org

C. File formats

File outputs are as described in section IV. The input file must be manually edited by the user in v1.0. However, a GUI may be introduced in later version.

D. Input file

```
#INPUT FILE input.py
ncore = 50 # number of cores for calculation
USE = "PYMATGEN" # PYMATGEN OR CIF
DFT = "ESPRESSO" #ESPRESSO, SIESTA, ABINIT, VASP
APIKEY = "YOURAPIKEY" #APIKEY for mat
MATERIALID = "mp-22866" # imput for pymatgen
SEEDNAME = "HB" #yours or default
SOC = True # TRUE or FALSE
KMESH = [8,8,8] # KMESH for nscf/wan
NUMBANDS = 120 # Number of bands
MAGNETISM = False
```

VI. WANNIER90 CONVERGENCE

Although all of the bands and energies are converged in the scf and nscf cycles there is the main issue of convergence with MLWFs that will cause most calculations to appear to not converge. A small error in the wannier minimization can lead to spurious bands that will lead to a non-real Fermi surface when conducting calculations with the results of that wannier90 run. There are many ways to correct this, such as iterating over many steps (>50,000), defining a good guess for the initial projection, changing the frozen window for disentanglement, etc. However, the main issue is two three fold, the initial projections (guess) must be manually defined or be made random, there should be an internal program that makes

good projection guesses from the known valence states and the result of the nscf run. Secondly, the steepest descent algorithm implemented in wannier90 v3.1 is not the best algorithm in order to get the proper minimization of the wannier centers. In fact, this method often gets stuck in local minimum during the calculation. Several better alternatives to the algorithm have been proposed but have not been implemented in the main wannier90 code³⁹⁻⁴¹. Finally, many of the interface codes to wannier90 were not written by the original developers of the respective DFT functions, this means that they could have many bugs or not correctly calculate the .mmn and .amn files needed for wannier90. This creates of problem of there being errors in wannier90 runs that must be corrected manually by users or are so fatal that wannier90 cannot parse to input file correctly at all. detracting from the possibility of ‘high throughput’ wannierization runs.

VII. EXAMPLES

In this section we present calculations utilizing the files that are generated by the programs. The only changes are made to the wannier90 input files in order to converge the MLWFs

A. 3D topological insulator Bi₂Se₃

Bi₂Se₃ has been discovered to be a 3D topological insulator^{29,30} with non-trivial surface states and an insulating bulk. Here we show a calculation utilizing quantum ESPRESSO with spin orbit coupling (SOC) on. Here we see the large Dirac cone at the Γ -point [Fig 1(A)]. In addition, we show the Fermi surface of the Dirac cone inside the band gap showing the topologically nontrivial surface states[Fig 1(B)].

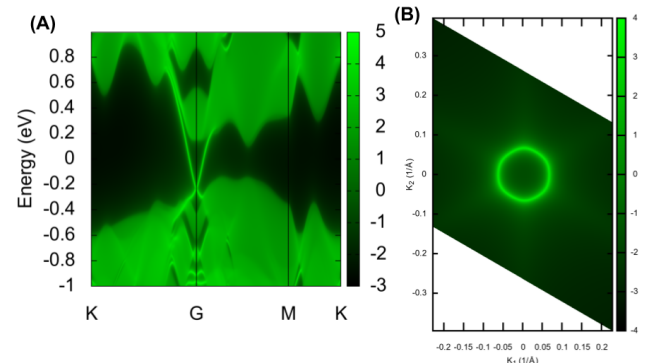


FIG. 1. Bi₂Se₃: (A) Surface states of the (001) surface (B) Fermi surface of Bi₂Se₃

B. Nodal line semimetal HfP₂

HfP₂ is a nodal line semimetal⁴² where the non-trivial state lies above the Fermi level in the presence of negligi-

ble spin-orbit coupling. although the nodal-line is above the Fermi surface non-trivial surface states that originate from the nodal line still exist throughout the band structure. The nodal-line is located about 0.2 eV above the Fermi level along the Γ -X line [Fig 2(A)]. We also show the Fermi surface of HfP_2 [Fig 2(B)].

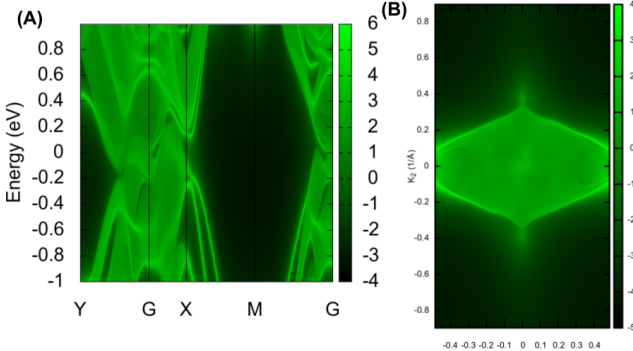


FIG. 2. HfP_2 : (A) Surface states of the (001) surface (B) Fermi surface of HfP_2

C. Weyl Semimetal TaAs

TaAs is the first material to be discovered to have a Weyl semimetal state. Weyl fermions materialize in condensed matter systems as chiral edge modes which are connected by Fermi arcs.

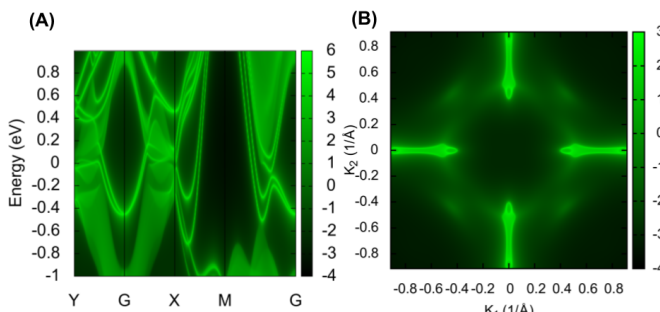


FIG. 3. TaAs : (A) Surface states of the (001) surface (B) Fermi surface of TaAs

VIII. CONCLUSION

In conclusion we have develop a program that can generate the input files needed to conduct calculations all the way for generating the wannier TB Hamiltonian and utilizing the result in wanniertools. Our program is designed to be easy to use at the expense of complexity and being able to input several settings into DFT programs. Currently, CIF2WAN can interface with quantum ESPRESSO, ABINIT, VASP, and SIESTA, with the

possibility of other quantum chemistry programs being added. In the future, we intend to add a graphical user interface once the program has been well tested.

IX. ACKNOWLEDGMENTS

The authors acknowledge the University of Central Florida Advanced Research Computing Center for providing computational resources and support that have contributed to results reported herein. URL: <https://arcc.ist.ucf.edu>.

Correspondence should be addressed to C.S (Email: Christophersims@knights.ucf.edu).

- ¹W. Kohn and L. J. Sham, *Physical Review* **140**, A1133 (1965).
- ²R. Jones, *Reviews of Modern Physics* **87**, 897 (2015).
- ³G. Kresse and J. Hafner, *Phys. Rev. B* **48**, 13115 (1993).
- ⁴J. P. Perdew, K. Burke, and M. Ernzerhof, *Phys. Rev. Lett.* **77**, 3865 (1996).
- ⁵X. Gonze, B. Amadon, P.-M. Anglade, J.-M. Beuken, F. Bottin, P. Boulanger, F. Bruneval, D. Caliste, R. Caracas, M. Côté, T. Deutsch, L. Genovese, P. Ghosez, M. Giantomassi, S. Goedecker, D. Hamann, P. Hermet, F. Jollet, G. Jomard, S. Leroux, M. Mancini, S. Mazevet, M. Oliveira, G. Onida, Y. Pouillon, T. Rangel, G.-M. Rignanese, D. Sangalli, R. Shaltaf, M. Torrent, M. Verstraete, G. Zerah, and J. Zwanziger, *Computer Physics Communications* **180**, 2582 (2009).
- ⁶X. Gonze, J.-M. Beuken, R. Caracas, F. Detraux, M. Fuchs, G.-M. Rignanese, L. Sindic, M. Verstraete, G. Zerah, F. Jollet, M. Torrent, A. Roy, M. Mikami, P. Ghosez, J.-Y. Raty, and D. Allan, *Computational Materials Science* **25**, 478 (2002).
- ⁷P. Giannozzi, O. Andreussi, T. Brumme, O. Bunau, M. B. Nardelli, M. Calandra, R. Car, C. Cavazzoni, D. Ceresoli, M. Cococcioni, N. Colonna, I. Carnimeo, A. D. Corso, S. de Gironcoli, P. Delugas, R. A. DiStasio, A. Ferretti, A. Floris, G. Fratesi, G. Fugallo, R. Gebauer, U. Gerstmann, F. Giustino, T. Gorni, J. Jia, M. Kawamura, H.-Y. Ko, A. Kokalj, E. Kçkbenli, M. Lazzeri, M. Marsili, N. Marzari, F. Mauri, N. L. Nguyen, H.-V. Nguyen, A. O. de-la Roza, L. Paulatto, S. Poncé, D. Rocca, R. Sabatini, B. Santra, M. Schlipf, A. P. Seitsonen, A. Smogunov, I. Timrov, T. Thonhauser, P. Umari, N. Vast, X. Wu, and S. Baroni, *Journal of Physics: Condensed Matter* **29**, 465901 (2017).
- ⁸P. Giannozzi, S. Baroni, N. Bonini, M. Calandra, R. Car, C. Cavazzoni, D. Ceresoli, G. L. Chiarotti, M. Cococcioni, I. Dabo, A. D. Corso, S. de Gironcoli, S. Fabris, G. Fratesi, R. Gebauer, U. Gerstmann, C. Gougaussis, A. Kokalj, M. Lazzeri, L. Martin-Samos, N. Marzari, F. Mauri, R. Mazzarello, S. Paolini, A. Pasquarello, L. Paulatto, C. Sbraccia, S. Scandolo, G. Sclauzero, A. P. Seitsonen, A. Smogunov, P. Umari, and R. M. Wentzcovitch, *Journal of Physics: Condensed Matter* **21**, 395502 (2009).
- ⁹J. M. Soler, E. Artacho, J. D. Gale, A. García, J. Junquera, P. Ordejón, and D. Sánchez-Portal, *Journal of Physics: Condensed Matter* **14**, 2745 (2002).
- ¹⁰P. Blaha, K. Schwarz, F. Tran, R. Laskowski, G. K. H. Madsen, and L. D. Marks, *The Journal of Chemical Physics* **152**, 074101 (2020).
- ¹¹N. Marzari and D. Vanderbilt, *Physical Review B* **56**, 12847 (1997).
- ¹²I. Souza, N. Marzari, and D. Vanderbilt, *Physical Review B* **65** (2001), 10.1103/physrevb.65.035109.
- ¹³N. Marzari, A. A. Mostofi, J. R. Yates, I. Souza, and D. Vanderbilt, *Reviews of Modern Physics* **84**, 1419 (2012).
- ¹⁴M. P. L. Sancho, J. M. L. Sancho, J. M. L. Sancho, and J. Rubio, *J. Phys. F: Met. Phys.* **15**, 851 (1985).
- ¹⁵A. Calzolari, N. Marzari, I. Souza, and M. B. Nardelli, *Physical Review B* **69** (2004), 10.1103/physrevb.69.035108.
- ¹⁶G. Pizzi, V. Vitale, R. Arita, S. Blgel, F. Freimuth, G. Géranton, M. Gibertini, D. Gresch, C. Johnson, T. Koretsune, J. Ibañez-Azpiroz, H. Lee, J.-M. Lihm, D. Marchand, A. Marrazzo, Y. Mokrousov, J. I. Mustafa, Y. Nohara, Y. Nomura, L. Paulatto,

- S. Poncé, T. Ponweiser, J. Qiao, F. Thle, S. S. Tsirkin, M. Wierzbowska, N. Marzari, D. Vanderbilt, I. Souza, A. A. Mostofi, and J. R. Yates, *Journal of Physics: Condensed Matter* **32**, 165902 (2020).
- ¹⁷Q. Wu, S. Zhang, H.-F. Song, M. Troyer, and A. A. Soluyanov, *Comput. Phys. Commun.* **224**, 405 (2018).
- ¹⁸R. P. Day, B. Zwartsenberg, I. S. Elfimov, and A. Damascelli, *npj Quantum Materials* **4** (2019), 10.1038/s41535-019-0194-8.
- ¹⁹T. Björkman, *Computer Physics Communications* **182**, 1183 (2011).
- ²⁰G. Pizzi, A. Cepellotti, R. Sabatini, N. Marzari, and B. Kozinsky, *Computational Materials Science* **111**, 218 (2016).
- ²¹A. Jain, S. P. Ong, G. Hautier, W. Chen, W. D. Richards, S. Dacek, S. Cholia, D. Gunter, D. Skinner, G. Ceder, and K. A. Persson, *APL Materials* **1**, 011002 (2013).
- ²²K. Choudhary, I. Kalish, R. Beams, and F. Tavazza, *Scientific Reports* **7** (2017), 10.1038/s41598-017-05402-0.
- ²³K. Choudhary, Q. Zhang, A. C. Reid, S. Chowdhury, N. V. Nguyen, Z. Trautt, M. W. Newrock, F. Y. Congo, and F. Tavazza, *Scientific Data* **5** (2018), 10.1038/sdata.2018.82.
- ²⁴K. Choudhary, G. Cheon, E. Reed, and F. Tavazza, *Physical Review B* **98** (2018), 10.1103/physrevb.98.014107.
- ²⁵K. Choudhary and F. Tavazza, *Computational Materials Science* **161**, 300 (2019).
- ²⁶K. Choudhary, K. F. Garrity, and F. Tavazza, *Scientific Reports* **9** (2019), 10.1038/s41598-019-45028-y.
- ²⁷K. Choudhary, K. F. Garrity, J. Jiang, R. Pachter, and F. Tavazza, [2001.11389v2](#).
- ²⁸M. Z. Hasan and C. L. Kane, *Rev. Mod. Phys.* **82**, 3045 (2010).
- ²⁹D. Hsieh, Y. Xia, D. Qian, L. Wray, F. Meier, J. Dil, J. Osterwalder, L. Patthey, A. Fedorov, H. Lin, *et al.*, *Phys. Rev. Lett.* **103**, 146401 (2009).
- ³⁰Y. Xia, D. Qian, D. Hsieh, L. Wray, A. Pal, H. Lin, A. Bansil, D. Grauer, Y. S. Hor, R. J. Cava, and M. Z. Hasan, *Nat. Phys.* **5**, 398 (2009).
- ³¹J. Hu, Z. Tang, J. Liu, X. Liu, Y. Zhu, D. Graf, K. Myhro, S. Tran, C. N. Lau, J. Wei, *et al.*, *Phys. Rev. Lett.* **117**, 016602 (2016).
- ³²L. M. Schoop, M. N. Ali, C. Straßer, A. Topp, A. Varykhalov, D. Marchenko, V. Duppel, S. S. P. Parkin, B. V. Lotsch, and C. R. Ast, *Nat. Commun.* **7**, 11696 (2016).
- ³³M. Neupane, I. Belopolski, M. M. Hosen, D. S. Sanchez, R. Sankar, M. Szwarc, S.-Y. Xu, K. Dimitri, N. Dhakal, P. Maldonado, P. M. Oppeneer, D. Kaczorowski, F. Chou, M. Z. Hasan, and T. Durakiewicz, *Phys. Rev. B* **93**, 201104(R) (2016).
- ³⁴M. M. Hosen, K. Dimitri, I. Belopolski, P. Maldonado, R. Sankar, N. Dhakal, G. Dhakal, T. Cole, P. M. Oppeneer, D. Kaczorowski, F. Chou, M. Z. Hasan, T. Durakiewicz, and M. Neupane, *Phys. Rev. B* **95**, 161101(R) (2017).
- ³⁵S.-Y. Xu, I. Belopolski, N. Alidoust, M. Neupane, G. Bian, C. Zhang, R. Sankar, G. Chang, Z. Yuan, C.-C. Lee, S.-M. Huang, H. Zheng, J. Ma, D. S. Sanchez, B. Wang, A. Bansil, F. Chou, P. P. Shibayev, H. Lin, S. Jia, and M. Z. Hasan, *Science* **349**, 613 (2015).
- ³⁶B. Q. Lv, H. M. Weng, B. B. Fu, X. P. Wang, H. Miao, J. Ma, P. Richard, X. C. Huang, L. X. Zhao, G. F. Chen, Z. Fang, X. Dai, T. Qian, and H. Ding, *Phys. Rev. X* **5**, 031013 (2015).
- ³⁷S.-M. Huang, S.-Y. Xu, I. Belopolski, C.-C. Lee, G. Chang, B. Wang, N. Alidoust, G. Bian, M. Neupane, C. Zhang, S. Jia, A. Bansil, H. Lin, and M. Z. Hasan, *Nat. Commun.* **6**, 7373 (2015).
- ³⁸G. H. Wannier, *Physical Review* **52**, 191 (1937).
- ³⁹J. I. Mustafa, S. Coh, M. L. Cohen, and S. G. Louie, *Physical Review B* **92** (2015), 10.1103/physrevb.92.165134.
- ⁴⁰A. Damle, A. Levitt, and L. Lin, [1801.08572v1](#).
- ⁴¹H. D. Cornean, D. Gontier, A. Levitt, and D. Monaco, *Annales Henri Poincaré* **20**, 1367 (2019).
- ⁴²C. Sims, M. M. Hosen, H. Aramberri, C.-Y. Huang, G. Dhakal, K. Dimitri, F. Kabir, S. Regmi, X. Zhou, T.-R. Chang, H. Lin, D. Kaczorowski, N. Kioussis, and M. Neupane, [1906.09642v1](#).

X. APPENDIX: Bi₂Se₃

A. BS.scf.in

```
&CONTROL
calculation = 'scf'
prefix = 'BS'
outdir = 'bin/'
pseudo_dir = 'PP/'
verbosity='high'
/

&system
ibrav = 0
nat = 5
ntyp = 2
ecutwfc = 60 !Ryberg
ecutrho = 500
occupations = 'smearing'
smearing = 'gaussian'
degauss = 0.01
/
!SOC
noncolin = .TRUE.
lspinorb = .TRUE.
starting_magnetization(1) = 0
starting_magnetization(2) = 0
/
&ELECTRONS
conv_thr = 1.0d-7
mixing_beta = 0.495
mixing_mode = 'TF'
diagonalization= 'david'
adaptive_thr=.true.
/
ATOMIC_SPECIES
Bi 208.9804 Bi.rel-pbesol-dn-kjpaw_psl.1.0.0.UPF
Se 78.96 Se.rel-pbesol-dn-kjpaw_psl.1.0.0.UPF
/
ATOMIC_POSITIONS (crystal)
Bi 0.3990 0.3990 0.6970
Bi 0.6010 0.6010 0.3030
Se 0.0000 0.0000 0.5000
Se 0.2060 0.2060 0.1180
Se 0.7940 0.7940 0.8820
/
CELL_PARAMETERS (angstrom)
-2.069 -3.583614 0.000000 ! crystal lattice
information
2.069 -3.583614 0.000000
0.000 2.389075 9.546667
/
K_POINTS (automatic)
8 8 1 1 1
```

B. BS.nscf.in

```

&CONTROL
calculation = 'nscf'
prefix = 'BS'
outdir = 'bin/'
pseudo_dir = 'PP/'
verbosity='high'
/

&system
ibrav = 0
nat = 5
ntyp = 2
ecutwfc =60 !Ryberg
ecutrho =500
occupations = 'smearing'
smearing = 'gaussian'
degauss = 0.01

nosym = .true.
nbnd = 200
!SOC
noncolin = .TRUE.
lspinorb = .TRUE.
starting_magnetization(1) = 0
starting_magnetization(2) = 0

/
&ELECTRONS
conv_thr = 1.0d-7
mixing_beta = 0.495
mixing_mode = 'TF'
diagonalization= 'david'
adaptive_thr=.true.
/

ATOMIC_SPECIES
Bi 208.9804 Bi.rel-pbesol-dn-kjpaw_psl.1.0.0.UPF
Se 78.96 Se.rel-pbesol-dn-kjpaw_psl.1.0.0.UPF

ATOMIC_POSITIONS (crystal)
Bi 0.3990 0.3990 0.6970
Bi 0.6010 0.6010 0.3030
Se 0.0000 0.0000 0.5000
Se 0.2060 0.2060 0.1180
Se 0.7940 0.7940 0.8820

CELL_PARAMETERS (angstrom)
-2.069 -3.583614 0.000000 ! crystal lattice
information
2.069 -3.583614 0.000000
0.000 2.389075 9.546667

K_POINTS (crystal)
64
0.00000000 0.00000000 0.00000000 1
0.00000000 0.00000000 0.25000000 1
0.00000000 0.00000000 0.50000000 1
0.00000000 0.00000000 0.75000000 1
0.00000000 0.25000000 0.00000000 1

```

```

0.00000000 0.25000000 0.25000000 1
0.00000000 0.25000000 0.50000000 1
0.00000000 0.25000000 0.75000000 1
0.00000000 0.50000000 0.00000000 1
0.00000000 0.50000000 0.25000000 1
0.00000000 0.50000000 0.50000000 1
0.00000000 0.50000000 0.75000000 1
0.00000000 0.75000000 0.00000000 1
0.00000000 0.75000000 0.25000000 1
0.00000000 0.75000000 0.50000000 1
0.00000000 0.75000000 0.75000000 1
0.00000000 0.75000000 0.75000000 1
0.25000000 0.00000000 0.00000000 1
0.25000000 0.00000000 0.25000000 1
0.25000000 0.00000000 0.50000000 1
0.25000000 0.00000000 0.75000000 1
0.25000000 0.25000000 0.00000000 1
0.25000000 0.25000000 0.25000000 1
0.25000000 0.25000000 0.50000000 1
0.25000000 0.25000000 0.75000000 1
0.25000000 0.50000000 0.00000000 1
0.25000000 0.50000000 0.25000000 1
0.25000000 0.50000000 0.50000000 1
0.25000000 0.50000000 0.75000000 1
0.25000000 0.50000000 0.00000000 1
0.25000000 0.50000000 0.25000000 1
0.25000000 0.50000000 0.50000000 1
0.25000000 0.50000000 0.75000000 1
0.25000000 0.75000000 0.00000000 1
0.25000000 0.75000000 0.25000000 1
0.25000000 0.75000000 0.50000000 1
0.25000000 0.75000000 0.75000000 1
0.25000000 0.75000000 0.75000000 1
0.50000000 0.00000000 0.00000000 1
0.50000000 0.00000000 0.25000000 1
0.50000000 0.00000000 0.50000000 1
0.50000000 0.00000000 0.75000000 1
0.50000000 0.25000000 0.00000000 1
0.50000000 0.25000000 0.25000000 1
0.50000000 0.25000000 0.50000000 1
0.50000000 0.25000000 0.75000000 1
0.50000000 0.50000000 0.00000000 1
0.50000000 0.50000000 0.25000000 1
0.50000000 0.50000000 0.50000000 1
0.50000000 0.50000000 0.75000000 1
0.50000000 0.75000000 0.00000000 1
0.50000000 0.75000000 0.25000000 1
0.50000000 0.75000000 0.50000000 1
0.50000000 0.75000000 0.75000000 1
0.50000000 0.75000000 0.75000000 1
0.75000000 0.00000000 0.00000000 1
0.75000000 0.00000000 0.25000000 1
0.75000000 0.00000000 0.50000000 1
0.75000000 0.00000000 0.75000000 1
0.75000000 0.25000000 0.00000000 1
0.75000000 0.25000000 0.25000000 1
0.75000000 0.25000000 0.50000000 1
0.75000000 0.25000000 0.75000000 1
0.75000000 0.50000000 0.00000000 1
0.75000000 0.50000000 0.25000000 1
0.75000000 0.50000000 0.50000000 1
0.75000000 0.50000000 0.75000000 1
0.75000000 0.75000000 0.00000000 1
0.75000000 0.75000000 0.25000000 1
0.75000000 0.75000000 0.50000000 1
0.75000000 0.75000000 0.75000000 1
0.75000000 0.75000000 0.75000000 1

```

C. BS.win

```

write_hr = .TRUE.
write_xyz = .TRUE.

```

```

!wannier_plot = .TRUE.
spinors = .TRUE.
num_wann = 50
dis_num_iter=1000
trial_step=50
num_iter=2000

exclude_bands = 1-50, 101-200

begin unit_cell_cart
-2.069 -3.583614 0.000000      ! crystal lattice
    information
 2.069 -3.583614 0.000000
 0.000  2.389075 9.546667
end unit_cell_cart

begin atoms_frac
 Bi 0.3990  0.3990  0.6970
 Bi 0.6010  0.6010  0.3030
 Se 0.0000  0.0000  0.5000
 Se 0.2060  0.2060  0.1180
 Se 0.7940  0.7940  0.8820
end atoms_frac

begin projections
random
end projections

begin kpoints

```

XI. APPENDIX: HfP₂

A. HfP2.scf.in

```

&CONTROL
calculation = 'scf'
prefix = 'HfP2'
outdir = './bin'
pseudo_dir = './PP/'
verbosity='high'
/

&system
ibrav = 0
nat = 12
ntyp = 2
ecutwfc = 50 !Ryberg
!occupations = 'tetrahedra_opt'
occupations = 'smearing'
smearing = 'gaussian'
degauss = 0.001

!SOC
noncolin = .FALSE.
lspinor = .FALSE.
starting_magnetization(1) = 0
starting_magnetization(2) = 0
/

&ELECTRONS

```

```

mixing_beta = 0.495
conv_thr = 1.0d-6
mixing_mode = 'TF'
diagonalization= 'david'
/
ATOMIC_SPECIES
P 30.974 P.upf
Hf 178.49 Hf.upf

ATOMIC_POSITIONS (crystal)
Hf 0.222920 0.750000 0.335788
Hf 0.777080 0.250000 0.664212
Hf 0.277080 0.250000 0.835788
Hf 0.722920 0.750000 0.164212
P 0.092791 0.750000 0.642458
P 0.907209 0.250000 0.357542
P 0.407209 0.250000 0.142458
P 0.592791 0.750000 0.857542
P 0.110700 0.750000 0.039379
P 0.889300 0.250000 0.960621
P 0.389300 0.250000 0.539379
P 0.610700 0.750000 0.460621

CELL_PARAMETERS (angstrom)
6.460131 0.000000 0.000000
0.000000 3.509322 0.000000
0.000000 0.000000 8.687298

K_POINTS (automatic)
8 8 8 0 0 0

```

B. HfP2.nscf.in

```

&CONTROL
calculation ='nscf'
prefix = 'HfP2'
outdir = './bin'
pseudo_dir = './PP/'
verbosity='high'
/
&system
ibrav = 0
nat = 12
ntyp = 2
ecutwfc = 50 !Ryberg
occupations = 'smearing'
smearing = 'gaussian'
degauss = 0.01
nosym = .TRUE.
nbnd = 120

!SOC
noncolin = .FALSE.
lspinorb = .FALSE.
starting_magnetization(1) = 0
starting_magnetization(2) = 0
/
&ELECTRONS
mixing_beta = 0.495
conv_thr = 1.0d-6
mixing_mode = 'TF'
diagonalization= 'david'
/
ATOMIC_SPECIES
P 30.974 P.upf
Hf 178.49 Hf.upf

ATOMIC_POSITIONS (crystal)
Hf 0.222920 0.750000 0.335788
Hf 0.777080 0.250000 0.664212
Hf 0.277080 0.250000 0.835788
Hf 0.722920 0.750000 0.164212
P 0.092791 0.750000 0.642458
P 0.907209 0.250000 0.357542
P 0.407209 0.250000 0.142458
P 0.592791 0.750000 0.857542
P 0.110700 0.750000 0.039379
P 0.889300 0.250000 0.960621
P 0.389300 0.250000 0.539379
P 0.610700 0.750000 0.460621

CELL_PARAMETERS (angstrom)
6.460131 0.000000 0.000000
0.000000 3.509322 0.000000
0.000000 0.000000 8.687298

K_POINTS (crystal)
512
0.0000000 0.0000000 0.00000000 1
0.0000000 0.0000000 0.12500000 1
0.0000000 0.0000000 0.25000000 1
0.0000000 0.0000000 0.37500000 1
0.0000000 0.0000000 0.50000000 1
0.0000000 0.0000000 0.62500000 1
0.0000000 0.0000000 0.75000000 1
0.0000000 0.0000000 0.87500000 1
0.0000000 0.12500000 0.00000000 1
0.0000000 0.12500000 0.12500000 1
0.0000000 0.12500000 0.25000000 1
0.0000000 0.12500000 0.37500000 1
0.0000000 0.12500000 0.50000000 1
0.0000000 0.12500000 0.62500000 1
0.0000000 0.12500000 0.75000000 1
0.0000000 0.12500000 0.87500000 1
0.0000000 0.25000000 0.00000000 1
0.0000000 0.25000000 0.12500000 1
0.0000000 0.25000000 0.25000000 1
0.0000000 0.25000000 0.37500000 1
0.0000000 0.25000000 0.50000000 1
0.0000000 0.25000000 0.62500000 1
0.0000000 0.25000000 0.75000000 1
0.0000000 0.25000000 0.87500000 1
0.0000000 0.37500000 0.00000000 1
0.0000000 0.37500000 0.12500000 1
0.0000000 0.37500000 0.25000000 1
0.0000000 0.37500000 0.37500000 1
0.0000000 0.37500000 0.50000000 1
0.0000000 0.37500000 0.62500000 1
0.0000000 0.37500000 0.75000000 1
0.0000000 0.37500000 0.87500000 1

```



```

0.75000000 0.25000000 0.62500000 0.87500000 0.37500000 0.00000000
0.75000000 0.25000000 0.75000000 0.87500000 0.37500000 0.12500000
0.75000000 0.25000000 0.87500000 0.87500000 0.37500000 0.25000000
0.75000000 0.37500000 0.00000000 0.87500000 0.37500000 0.37500000
0.75000000 0.37500000 0.12500000 0.87500000 0.37500000 0.50000000
0.75000000 0.37500000 0.25000000 0.87500000 0.37500000 0.62500000
0.75000000 0.37500000 0.37500000 0.87500000 0.37500000 0.75000000
0.75000000 0.37500000 0.50000000 0.87500000 0.37500000 0.87500000
0.75000000 0.37500000 0.62500000 0.87500000 0.50000000 0.00000000
0.75000000 0.37500000 0.75000000 0.87500000 0.50000000 0.12500000
0.75000000 0.37500000 0.87500000 0.87500000 0.50000000 0.25000000
0.75000000 0.50000000 0.00000000 0.87500000 0.50000000 0.37500000
0.75000000 0.50000000 0.12500000 0.87500000 0.50000000 0.50000000
0.75000000 0.50000000 0.25000000 0.87500000 0.50000000 0.62500000
0.75000000 0.50000000 0.37500000 0.87500000 0.50000000 0.75000000
0.75000000 0.50000000 0.50000000 0.87500000 0.50000000 0.87500000
0.75000000 0.50000000 0.62500000 0.87500000 0.62500000 0.00000000
0.75000000 0.50000000 0.75000000 0.87500000 0.62500000 0.12500000
0.75000000 0.50000000 0.87500000 0.87500000 0.62500000 0.25000000
0.75000000 0.62500000 0.00000000 0.87500000 0.62500000 0.37500000
0.75000000 0.62500000 0.12500000 0.87500000 0.62500000 0.50000000
0.75000000 0.62500000 0.25000000 0.87500000 0.62500000 0.62500000
0.75000000 0.62500000 0.37500000 0.87500000 0.62500000 0.75000000
0.75000000 0.62500000 0.50000000 0.87500000 0.62500000 0.87500000
0.75000000 0.62500000 0.62500000 0.87500000 0.75000000 0.00000000
0.75000000 0.62500000 0.75000000 0.87500000 0.75000000 0.12500000
0.75000000 0.62500000 0.87500000 0.87500000 0.75000000 0.25000000
0.75000000 0.75000000 0.00000000 0.87500000 0.75000000 0.37500000
0.75000000 0.75000000 0.12500000 0.87500000 0.75000000 0.50000000
0.75000000 0.75000000 0.25000000 0.87500000 0.75000000 0.62500000
0.75000000 0.75000000 0.37500000 0.87500000 0.75000000 0.75000000
0.75000000 0.75000000 0.50000000 0.87500000 0.75000000 0.87500000
0.75000000 0.75000000 0.62500000 0.87500000 0.87500000 0.87500000
end kpoints

```

XII. APPENDIX: HfP₂

A. TA.scf.in

```

&CONTROL
calculation = 'scf'
prefix = 'TA'
outdir = './bin'
pseudo_dir = './PP/'
verbosity='high'
/

&system
ibrav = 0
nat = 4
ntyp = 2
ecutwfc =55 !Ryberg
ecutrho =550
occupations = 'smearing',
smearing = 'mv'
degauss = 0.002

```

```

!SOC
noncolin = .TRUE.
lspinorb = .TRUE.
starting_magnetization(1) = 0
starting_magnetization(2) = 0

/
&ELECTRONS
conv_thr = 1.0d-7
mixing_beta = 0.495
diagonalization= 'david'
adaptive_thr=.true.
/

ATOMIC_SPECIES
Ta 180.94788 Ta_ONCV_PBE_fr.upf
As 74.9216 As_ONCV_PBE_fr.upf

ATOMIC_POSITIONS (crystal)
Ta 0.25000 0.75000 0.50000
Ta 0.00000 0.00000 0.00000
As 0.66700 0.16700 0.33400
As 0.41700 0.41700 0.83400

CELL_PARAMETERS (angstrom)
3.437000 -0.000000 -0.000000
-0.000000 3.437000 0.000000
-1.718500 -1.718500 5.828000

K_POINTS (automatic)
8 8 8 0 0 0


---


B. TA.nscf.in



---


&CONTROL
calculation ='nscf'
prefix = 'TA'
outdir = './bin'
pseudo_dir = './PP/'
verbosity='high'
/
&system
ibrav = 0
nat = 4
ntyp = 2
ecutwfc =55 !Ryberg
ecutrho =550
!occupations = 'fixed'
occupations = 'smearing'
smearing = 'mv'
degauss = 0.002
nosym = .true.
nbnd = 120
!SOC
noncolin = .TRUE.
lspinorb = .TRUE.
starting_magnetization(1) = 0
starting_magnetization(2) = 0

/
&ELECTRONS
conv_thr = 1.0d-7
mixing_beta = 0.495
diagonalization= 'david'
adaptive_thr=.true.
/

ATOMIC_SPECIES
Ta 180.94788 Ta_ONCV_PBE_fr.upf
As 74.9216 As_ONCV_PBE_fr.upf

ATOMIC_POSITIONS (crystal)
Ta 0.25000 0.75000 0.50000
Ta 0.00000 0.00000 0.00000
As 0.66700 0.16700 0.33400
As 0.41700 0.41700 0.83400

CELL_PARAMETERS (angstrom)
3.437000 -0.000000 -0.000000
-0.000000 3.437000 0.000000
-1.718500 -1.718500 5.828000

K_POINTS (crystal)
64
0.0000000 0.0000000 0.0000000 1
0.0000000 0.0000000 0.2500000 1
0.0000000 0.0000000 0.5000000 1
0.0000000 0.0000000 0.7500000 1
0.0000000 0.2500000 0.0000000 1
0.0000000 0.2500000 0.2500000 1
0.0000000 0.2500000 0.5000000 1
0.0000000 0.2500000 0.7500000 1
0.0000000 0.5000000 0.0000000 1
0.0000000 0.5000000 0.2500000 1
0.0000000 0.5000000 0.5000000 1
0.0000000 0.5000000 0.7500000 1
0.0000000 0.5000000 0.7500000 1
0.0000000 0.7500000 0.0000000 1
0.0000000 0.7500000 0.2500000 1
0.0000000 0.7500000 0.5000000 1
0.0000000 0.7500000 0.7500000 1
0.2500000 0.0000000 0.0000000 1
0.2500000 0.0000000 0.2500000 1
0.2500000 0.0000000 0.5000000 1
0.2500000 0.0000000 0.7500000 1
0.2500000 0.2500000 0.0000000 1
0.2500000 0.2500000 0.2500000 1
0.2500000 0.2500000 0.5000000 1
0.2500000 0.2500000 0.7500000 1
0.2500000 0.5000000 0.0000000 1
0.2500000 0.5000000 0.2500000 1
0.2500000 0.5000000 0.5000000 1
0.2500000 0.5000000 0.7500000 1
0.2500000 0.7500000 0.0000000 1
0.2500000 0.7500000 0.2500000 1
0.2500000 0.7500000 0.5000000 1
0.2500000 0.7500000 0.7500000 1
0.5000000 0.0000000 0.0000000 1

```



```
0.75000000 0.75000000 0.50000000  
0.75000000 0.75000000 0.75000000
```

```
end kpoints
```